Vision-based Control Laws for Distributed Flocking of Nonholonomic Agents

Nima Moshtagh, Ali Jadbabaie, Kostas Daniilidis

GRASP Laboratory, University of Pennsylvania, Philadelphia, PA 19104
Email: {nima, jadbabai, kostas}@grasp.upenn.edu

Abstract— **We study the problem of vision-based flocking and coordination of a group of kinematic agents in 2 and 3 dimensions. It is shown that in the absence of communication among agents, and by using only visual information, a group of mobile agents can align their velocity vectors and move in a formation. A coordinate-free control law is used to develop a vision-based input for each nonholonomic agent. The vision-based input does not rely on heading measurements, but only requires measurements of bearing, optical flow and time-to-collision, all of which can be efficiently measured.**

I. INTRODUCTION

Cooperative control of multiple autonomous agents has become a vibrant part of control theory research. The main underlying theme of this line of research is to analyze and/or synthesize spatially distributed control architectures that can be used for motion coordination of large groups of autonomous vehicles. Each vehicle is assumed to be capable of local sensing and communication, and there is often a global objective, such as swarming, or reaching a stable formation, etc. Some of the relevant research in control theory and robotics are [2], [9], [12], [16], [19].

Many of the existing vision-based distributed control strategies assume that the robots are capable of communicating an estimation of their position with their neighbors [17], [21], [22] and are based on distributed computation [1]. Other cooperative systems based on local computation work in the configuration space [7], [15]. From the vision point of view, our approach is similar to visual versoing methods used in [5], [6], [18]. However, these approaches assume that a specific vertical pose of an omnidirectional camera allows the computation of both bearing and distance, while we use only bearing, the optical flow (bearing derivative), and time-to-collision.

In the work of Cowan *et al.* [5] the formation control problem is considered as a visual servoing task. For a pair of mobile robots denoted as leader and follower, it is assumed that the follower can measure a pair of features on the leader. The relative kinematics of the leader and the follower in the image plane is derived, and by using feedback linearization string stability and leader-to-formation stability is achieved.

In [6] a framework for vision-based formation control of a group of nonholonomic mobile robots is proposed. The two features in their approach is first using the omnidirectional cameras as the only sensor for the robots, and second a decentralized controller that allows for changes in the formation. The images from the omnidirectional cameras are used to estimate the relative angle and distances between agents. Then, by applying input-output feedback linearization they designed control laws for leader following and obstacle avoidance.

While the nearest neighbor interactions have been shown to be biologically plausible and have been observed in schools of fish and flocks of birds, the assumptions about knowledge of relative headings and distances is not biologically plausible. Even if some species might use ultrasound to estimate distances or binocular vision to estimate positions and motions of others, such sensing mechanisms do not perform well for flocking where simultaneous measurements in multiple directions are needed. The simplest assumption we can make is that such systems have only monocular vision and that they have basic visual capabilities like the estimation of *optical flow* and *time to collision*. Experimental evidence suggest that several animal species, including pigeons, are capable of estimating time to collision [11], [20]. Computationally, time to collision can be estimated from the ratio of area change to area or from the divergence of the optical flow [4], [10]. Regarding optical flow, we refer the reader to the survey [3].

Based on the idea of a *geodesic control law* [14], which results in velocity alignment of a group of agents in 2D and 3D, we generate a control algorithm that uses only visual clues from images. Similar to [5] we approach the formation control problem as a visual versoing task. We write the equation of motion for each agent, and solve it for the input controllers. Since we are *not* assuming that the relative distance measurements are available, we are able to extend our results to motion in three dimensional space. Also, we generalize the solutions of the equations of motion to multiple agents.

In Section II we introduce a coordinate-free control law for velocity alignment. We derive the optical flow equation for a group of agents in section III. In Sections IV and V the control law and the optical flow equation are used to develop a vision-based control law for flocking in 2D and 3D that only needs the measurements of bearing, optical flow and time-to-collision. Finally, in Section VI we numerically verify the correctness of our vision-based controllers.

II. GEODESIC CONTROL LAWS

Consider a group of N agents in the 3 dimensional space. Each agent is capable of sensing some information from its neighbors as defined by

$$\mathcal{N}_i \doteq \{j | i \sim j\} \subseteq \{1, \ldots, N\} \backslash \{i\}. \quad (1)$$

The neighborhood set of agent i, $\mathcal{N}_i$, is a set of agents that can be "seen" by agent i. The precise meaning of "seeing" will be cleared later in section IV. The size of the neighborhood depends on the characteristics of the sensors. Our goal in this section is to design a control law for each agent to drive the multi-agent system to the consensus state.

*Definition 2.1: (**Consensus State**) The state where all the headings are the same is called the consensus state.*

Without loss of generality, it is assumed that all agents are kinematic agents and move with a constant unit speed i.e $|v_i| = 1, \ i \in \{1, \ldots, N\}$. Let the rotation matrix $R_i = [R_{ix}, R_{iy}, R_{iz}]$ represent the attitude of agent i in the fixed world frame (R_{ik} is the k-th column of matrix R_i). We have assumed the velocity vector v_i is along the third column of the attitude matrix (or along the z-axis of the body frame), so we have $v_i = R_i e_3$ where $e_3 = [0, 0, 1]^T$. Using the kinematic equation $\dot{R}_i = R_i \hat{\omega}_i$ where $\omega_i = [\omega_{ix}, \omega_{iy}, \omega_{iz}]^T$ is the body angular velocity expressed in the body frame of agent i and

$$\hat{\omega}_i = \begin{bmatrix} 0 & -\omega_{iz} & \omega_{iy} \\ \omega_{iz} & 0 & -\omega_{ix} \\ -\omega_{iy} & \omega_{ix} & 0 \end{bmatrix},$$

we write the kinematics of the system as

$$\dot{v}_i = \dot{R}_i e_3 = R_i \hat{\omega}_i e_3 \quad i = 1, \ldots, N$$

which can be simplified to

$$\dot{v}_i = -\omega_{ix} R_{iy} + \omega_{iy} R_{ix} \quad i = 1, \ldots, N. \quad (2)$$

System (2) is an underactuated system with control inputs ω_{ix} and ω_{iy}. Note that ω_{iz} is free, which implies that we do not directly control the torsion or rotation around v_i (see Figure 1). We choose the control input ω_i of the form

$$\omega_i = \sum_{j \in \mathcal{N}_i} \frac{1}{l_{ij}} (v_i \times v_j) \quad (3)$$

where l_{ij} is the distance between agents i and j. Input (3) is a coordinate-free control input, because it is in terms of v_i and v_j, expressed the body-frame of agent i. Since the velocity of agent i in its own frame is $v_i = [0, 0, 1]^T$, we have

$$\omega_i = \sum_{j \in \mathcal{N}_i} \frac{1}{l_{ij}} \begin{bmatrix} -v_{jy} \\ v_{jx} \\ 0 \end{bmatrix} = \sum_{j \in \mathcal{N}_i} \frac{1}{l_{ij}} \begin{bmatrix} -< v_j, R_{iy} > \\ < v_j, R_{ix} > \\ 0 \end{bmatrix}.$$

As shown in [13], the above control law is a *geodesic control law* that minimizes the following misalignment potential

$$V = \frac{1}{2} \sum_{i \sim j} \|v_i - v_j\|^2$$

where the summation is over all the neighboring agents. The above geodesic control input results in the alignment of the velocity vectors, as long as the underlying proximity graph of the multi-agent system remains connected. Thus, the consensus state is an stable equilibrium of the system. As mentioned in [13], there are other stable equilibria besides all the velocity vectors being equal. In summary, we have the following theorem:

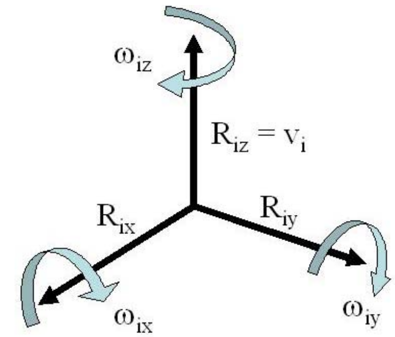

Fig. 1. angular velocity

Theorem 2.2: Consider the system of N kinematic equations $\dot{v}_i = -\omega_{ix} R_{iy} + \omega_{iy} R_{ix}, \ i = 1, \ldots, N$. If the proximity graph of the agents is fixed and connected, then by applying the control law

$$\omega_i = \sum_{j \in \mathcal{N}_i} \frac{1}{l_{ij}} (v_i \times v_j) \quad (4)$$

all trajectories converge to the equilibria given by $\omega_i = 0$. Furthermore, the consensus state is locally asymptotically stable.

III. Optical Flow Equation

Let $j \in \mathcal{N}_i$ be a neighbor of agent i. In the body-frame of agent i, the relative position of agents i and j can be represented by a vector $Q_{ij} \in \mathbb{R}^3$ as shown in Figure 3. The equation of relative motion for a pair of agents i and j is derived in Appendix A, and is given by

$$\dot{Q}_{ij} = -\omega_i \times Q_{ij} + (v_j - v_i) \quad (5)$$

where $\omega_i \in \mathbb{R}^3$ is the angular velocity vector of agent i, and v_i and v_j are the velocity vectors of agents i and j respectively, all given in the body-frame of agent i.

Let l_{ij} denote the distance between agents i and j. We normalize the optical flow equation (5) by dividing it by l_{ij} to get

$$\dot{Q}_{ij}/l_{ij} = -\omega_i \times q_{ij} + \frac{1}{l_{ij}}(v_j - v_i), \quad \forall j \in \mathcal{N}_i \quad (6)$$

where $q_{ij} = Q_{ij}/l_{ij}$ is the unit-length bearing vector. Equation (6) holds for all the agents that are in $\mathcal{N}_i$. Thus, we sum (6) over all $j \in \mathcal{N}_i$ to get:

$$\sum_{j \in \mathcal{N}_i} \dot{Q}_{ij}/l_{ij} = -\sum_{j \in \mathcal{N}_i} \omega_i \times q_{ij} + \sum_{j \in \mathcal{N}_i} \frac{1}{l_{ij}}(v_j - v_i) \quad (7)$$

The goal is to solve (7) for input ω_i so that it is only a function of some measurable quantities such as bearing and time-to-collision.

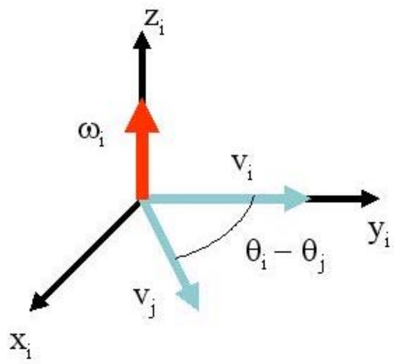

Fig. 2. Vectors v_i, v_j and ω_i in the special case of planar motion.

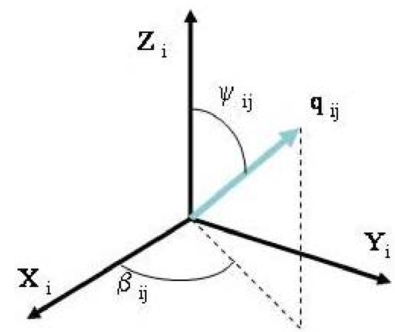

Fig. 3. The polar angle β_{ij} and the azimuth ψ_{ij} for two agents in 3D.

IV. Vision-based Planar Formation

When nonholonomic robots move on the plane, we can model their motion with unicycle kinematic agents. It is assumed that all agents move with constant unit speed. Thus, for each agent the kinematic model becomes:

$$\begin{aligned} \dot{x}_i &= \cos\theta_i \\ \dot{y}_i &= \sin\theta_i \\ \dot{\theta}_i &= \omega_i \qquad i = 1, \ldots, N \ . \end{aligned} \tag{8}$$

When we restrict the motion of agents to plane $z = 0$, the control law presented in section II will reduce to

$$\omega_{ix} = \omega_{iy} = 0, \quad \omega_{iz} = -\sum_{j\in\mathcal{N}_i} \frac{1}{l_{ij}} \sin(\theta_i - \theta_j) \tag{9}$$

which results in velocity alignment in a multi-agent system [8]. In this section we use this control law to solve the optical flow equation (7) for ω_i so that it is only in terms of the measurable quantities.

For planar agents, the horizontal bearing β_{ij} is defined by the angle that the projection of agent j makes with the body-frame of agent i, and is given by:

$$\beta_{ij} = \text{atan2}\big(y_j - y_i\ ,\ x_j - x_i\big) - \theta_i + \frac{\pi}{2} \tag{10}$$

and its rate of change $\dot{\beta}_{ij}$ defines the optical flow. It can be shown that the time-to-collision between agents i and j can be measured as the rate of growth of the image area [11], i.e. the relative change in the area A_{ij} of projection of agent j on the image plane of agent i. In other words

$$\tau_{ij} = \frac{A_{ij}}{\dot{A}_{ij}} = \frac{l_{ij}}{\dot{l}_{ij}}. \tag{11}$$

To formally define the sensing, we assume that each agent i can measure:

- β_{ij} or the relative bearing in agent i's reference frame
- $\dot{\beta}_{ij}$ or "optical flow": the rate of change of bearing
- τ_{ij} or "time-to-collision"

for any agent j in the set of its neighbors $\mathcal{N}_i$.

For robots moving on the ground, the solution of the optical flow equation (7) can be obtained by substituting values for q_{ij}, ω_i, v_i and v_j restricted to the planar motion (corresponding to plane $z = 0$). The body-frame of agent i is such that the velocity vector v_i is along the y-axis, and the angular velocity ω_i is orthogonal to the (x, y)-plane (see Figure 2). Thus

$$v_i = [0,\ 1,\ 0]^T \qquad \omega_i = [0,\ 0,\ \omega_{iz}]^T.$$

The bearing vector Q_{ij} and the velocity vector v_j of a neighboring agent in the body-frame of agent i becomes

$$Q_{ij} = \begin{bmatrix} l_{ij}\ \cos\beta_{ij} \\ l_{ij}\ \sin\beta_{ij} \\ 0 \end{bmatrix}, \qquad v_j = \begin{bmatrix} \sin(\theta_i - \theta_j) \\ \cos(\theta_i - \theta_j) \\ 0 \end{bmatrix}$$

where β_{ij} is the bearing angle. A simple differentiation of Q_{ij} reveals that we have $\dot{Q}_{ij} = M_{ij}\ Q_{ij}$ where M_{ij} is the *measurement matrix*, and is given by:

$$M_{ij} = \begin{bmatrix} 1/\tau_{ij} & -\dot{\beta}_{ij} & 0 \\ \dot{\beta}_{ij} & 1/\tau_{ij} & 0 \\ 0 & 0 & 1/\tau_{ij} \end{bmatrix}.$$

By substituting for v_i, v_j, ω_i and q_{ij} in (7) we get:

$$\sum_{j\in\mathcal{N}_i} M_{ij}\ q_{ij} = -\begin{bmatrix} 0 \\ 0 \\ \omega_{iz} \end{bmatrix} \times \sum_{j\in\mathcal{N}_i} q_{ij} + \sum_{j\in\mathcal{N}_i} \frac{1}{l_{ij}} \begin{bmatrix} \sin(\theta_i - \theta_j) \\ \cos(\theta_i - \theta_j) \\ -1 \end{bmatrix}.$$

Out of the three linear equations we obtained only the first one is used to solve for ω_{iz}, and by using (9) we get

$$\omega_{iz} = \frac{\sum_{j\in\mathcal{N}_i} \left(\dot{\beta}_{ij}\sin\beta_{ij} - \frac{1}{\tau_{ij}}\cos\beta_{ij}\right)}{1 - \sum_{j\in\mathcal{N}_i}\sin\beta_{ij}}. \tag{12}$$

This is the vision-based control law that is equivalent to (9) and gives us velocity alignment for a group of kinematic agents. See section VI for simulations that show the effectiveness of this vision-based control input.

V. Vision-Based Formation Control in 3D

Consider a group of N agents in the 3 dimensional space. Each agent is capable of sensing some information from its neighbors as defined by (1). Similar assumptions on the neighborhood relationships hold as explained in section II. In three dimensions, the location of agent i in a fixed world coordinates is given by (x_i, y_i, z_i) and its velocity is $v_i = (\dot{x}_i, \dot{y}_i, \dot{z}_i)^T$.

Let q_{ij} be a unit vector starting from agent i and pointing towards agent j, as shown in Figure 3. The bearing of agent j with respect to agent i is the projection of agent j and is represented by a pair of angles (β_{ij}, ψ_{ij}). The polar angle β_{ij} is given by the angle between projection of q_{ij} and the x-axis of agent i's body frame and the azimuth angle ψ_{ij} is given by the angle between the vector q_{ij} and the z-axis of agent i's body frame:

$$\beta_{ij} = \text{atan2}\big(y_j - y_i\ ,\ x_j - x_i\big) - \theta_i + \frac{\pi}{2} \quad (13)$$

$$\psi_{ij} = \frac{\pi}{2} - \phi_i - \text{atan2}\big(r_{ij}\ ,\ z_j - z_i\big) \quad (14)$$

where $r_{ij} = \sqrt{(y_j - y_i)^2 + (x_j - x_i)^2}$.

The speed of projection is the optical flow and is given by the rate of change of bearing ($\dot{\beta}_{ij}$, $\dot{\psi}_{ij}$), and time-to-collision between agents i and j can be measured as in (11). In summary, each agent i can measure:

- $(\beta_{ij},\ \psi_{ij})$ as the bearing angles
- $(\dot{\beta}_{ij},\ \dot{\psi}_{ij})$ as the optical flow
- τ_{ij} or "time-to-collision"

for any agent j in the set of neighbors $\mathcal{N}_i$.

For a group of agents moving in the 3-dimensional space, a controller that results in velocity alignment is the one that steers the headings and attitudes of all the agents to a common value. In what follows, we use the control law (4) to solve the optical flow equation (7). By solving the above equation we mean finding an expression for vector ω_i that is only a function of the measurable quantities.

Next, we show how we can write the terms of optical flow equation in terms of either inputs or measurable quantities.

1) Position Vector Q_{ij}: The position vector $Q_{ij} \in \mathbb{R}^3$ is given by

$$Q_{ij} = \begin{bmatrix} l_{ij}\sin\psi_{ij}\cos\beta_{ij} \\ l_{ij}\sin\psi_{ij}\sin\beta_{ij} \\ l_{ij}\cos\psi_{ij} \end{bmatrix}. \quad (15)$$

A simple differentiation of Q_{ij} shows that $\dot{Q}_{ij} = M_{ij}Q_{ij}$ where the *measurement matrix* M_{ij} is given by

$$M_{ij} = \begin{bmatrix} 1/\tau_{ij} & -\dot{\beta}_{ij} & \dot{\psi}_{ij}\cos\beta_{ij} \\ \dot{\beta}_{ij} & 1/\tau_{ij} & \dot{\psi}_{ij}\sin\beta_{ij} \\ -\dot{\psi}_{ij}\cos\beta_{ij} & -\dot{\psi}_{ij}\sin\beta_{ij} & 1/\tau_{ij} \end{bmatrix}.$$

Thus, we have the left-hand-side of (7) in terms of the measurements:

$$\sum_{j\in\mathcal{N}_i} \dot{Q}_{ij}/l_{ij} = \sum_{j\in\mathcal{N}_i} M_{ij}q_{ij} \quad (16)$$

2) Relative velocity $(v_i - v_j)$: Given $v_i = [0, 0, 1]^T$ and $v_j = [v_{jx}, v_{jy}, v_{jz}]^T$ the control input (4) becomes

$$\omega_i = \sum_{j\in\mathcal{N}_i} \frac{1}{l_{ij}}(v_i \times v_j) = \sum_{j\in\mathcal{N}_i} \frac{1}{l_{ij}} \begin{bmatrix} -v_{jy} \\ v_{jx} \\ 0 \end{bmatrix} = \begin{bmatrix} \omega_{ix} \\ \omega_{iy} \\ 0 \end{bmatrix}$$

Now, we write the relative velocities in terms of the inputs ω_{iy} and ω_{ix}.

$$\sum_{j\in\mathcal{N}_i} \frac{1}{l_{ij}}(v_j - v_i) = \sum_{j\in\mathcal{N}_i} \frac{1}{l_{ij}} \begin{bmatrix} v_{jx} \\ v_{jy} \\ v_{jz} - 1 \end{bmatrix} = \begin{bmatrix} \omega_{iy} \\ -\omega_{ix} \\ \sum_j \frac{1}{l_{ij}}(v_{jz} - 1) \end{bmatrix}. \quad (17)$$

As we will see, the third element has no effect on our solution, so we leave it as it is.

3) Solving The Optical Flow Equation: Now, we have every term in (7) in terms of either the input ω_i or the measurable quantities. We plug in (16) and (17) into optical flow equation, which we repeat here:

$$\sum_{j\in\mathcal{N}_i} \dot{Q}_{ij}/l_{ij} = -\sum_{j\in\mathcal{N}_i} \omega_i \times q_{ij} + \sum_{j\in\mathcal{N}_i} \frac{1}{l_{ij}}(v_j - v_i).$$

After substitution we have

$$\sum_{j\in\mathcal{N}_i} M_{ij}q_{ij} = -\begin{bmatrix} \omega_{ix} \\ \omega_{iy} \\ 0 \end{bmatrix} \times \sum_{j\in\mathcal{N}_i} q_{ij} + \begin{bmatrix} \omega_{iy} \\ -\omega_{ix} \\ \dots \end{bmatrix}.$$

The above gives us 3 linear equations in terms of the input and our measurements, but only the first two are used to solve for the control inputs. By solving the first two equations for ω_{ix} and ω_{iy} we get

$$\omega_{ix} = \frac{-(\sum_j M_{ij}q_{ij})_2}{1 - \sum_{j\in\mathcal{N}_i}\cos\psi_{ij}} \quad (18)$$

$$\omega_{iy} = \frac{(\sum_j M_{ij}q_{ij})_1}{1 - \sum_{j\in\mathcal{N}_i}\cos\psi_{ij}} \quad (19)$$

where the numerators are

$$\begin{aligned} \big(\sum_{j\in\mathcal{N}_i} M_{ij}q_{ij}\big)_1 &= \frac{1}{\tau_{ij}}\sin\psi_{ij}\cos\beta_{ij} - \dot{\beta}_{ij}\sin\psi_{ij}\sin\beta_{ij} \\ &+ \dot{\psi}_{ij}\cos\psi_{ij}\cos\beta_{ij} \\ \big(\sum_{j\in\mathcal{N}_i} M_{ij}q_{ij}\big)_2 &= \frac{1}{\tau_{ij}}\sin\psi_{ij}\sin\beta_{ij} + \dot{\beta}_{ij}\sin\psi_{ij}\cos\beta_{ij} \\ &+ \dot{\psi}_{ij}\cos\psi_{ij}\sin\beta_{ij}. \end{aligned}$$

Therefore, equations (18) and (19) are the vision-based control inputs. They are only in terms of the measured quantities of bearing, optical flow and time-to-collision, as desired. In section VI we numerically show the vision-based control laws result in a stable flocking according to definition 2.1.

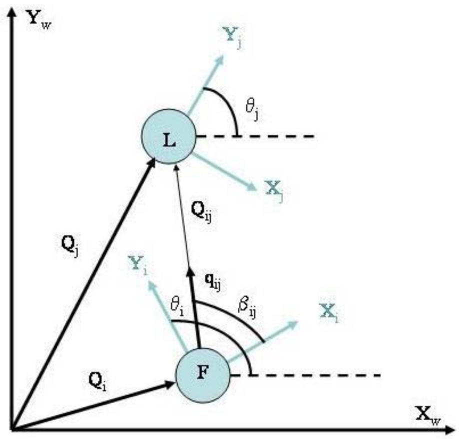

Fig. 4. Configuration of two agents.

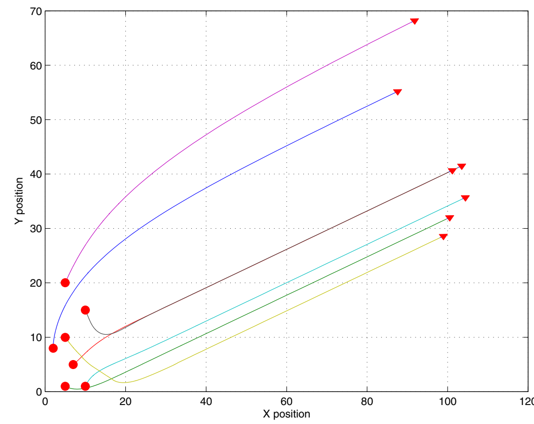

Fig. 5. 7 agents flock in 2D.

VI. Simulations

To numerically verify our theory of vision-based formation control, a *Simulink* simulation was made. For each agent the required measurements were numerically computed. From (13) and (14) the bearing β_{ij} and attitude ψ_{ij} were computed and by numerically differentiating them the optical flow was computed. Also, equation (11) was used to compute time-to-collision τ_{ij} between two agents.

Figure 5 shows that in a planar motion seven agents can align their velocity vectors by using vision-based control law (12). The proximity graph is not complete, i.e. not every agent can "see" every other agent. In Figure 6, four kinematic agents align their velocity vectors in 3D by using vision-based control laws (18) and (19) and achieve a stable formation.

We can designate one of the agents to be the leader of the group. It was proved in [14] that in the presence of a leader all other agents (followers) are forced to align their velocities with that of the leader. Figure 7 shows an example of a leader-following using vision-based control laws with a dynamic leader. All agents follow the leader moving in a sinusoidal path.

In a real experiment, the measurements of the bearing angles and time-to-collision will include noise. The noise will be amplified when we differentiate the bearing to compute the optical flow. To study the effect of noise on our vision-based flocking, a Gaussian random noise was added to the measurements of bearing.

Figure 8.a shows five agents, in the noise-free case. The heading of all agents in plotted in Figure 8.b. Addition of the noise to the measurements of the bearing decreases the rate of convergence, as it can be seen in Figures 8.c and 8.d.

VII. Conclusions

We have developed control laws for nonholonomic robots that only use visual measurements from cameras for velocity alignment. We saw that these vision-based controllers only need the values of bearing, optical flow and time-to-collision, all of which can be measured from images. The designed control laws are distributed and can be used for velocity alignment in multi-agent systems.

The experiments on real robots is an ongoing work. A series of Evolution Robots (ER) robots are being used to verify the theory. Each robot is equipped with a camera that has a fish-eye lens capable of seeing the entire surrounding of the robot (with a field of view of 360 degrees). The challenging part of the experiment is making accurate measurements of optical flow and time-to-collision in the presence of noise in the images. Both quantities require differentiating noisy measurements that will amplify the noise and increase the error.

VIII. Appendices

In Appendix A we derive the equation of motion (5).

A. *Equation of Motion*

Let ${}^b(\cdot)$ denote a vector in the body frame of agent i and ${}^f(\cdot)$ a vector in the fixed world frame. Let $j \in \mathcal{N}_i$ be any neighbor of agent i. As shown in Figure 4 the relative position of agents i and j can be represented by a vector ${}^bQ_{ij} \in \mathbb{R}^3$:

$${}^bQ_{ij} = ({}^bR_f)({}^fQ_{ij})$$

where ${}^bR_f$ is the rotation matrix from the fixed frame to the body frame. Since $\dot{Q}_{ij} = \dot{Q}_j - \dot{Q}_i = v_j - v_i$, by differentiating Q_{ij} with respect to time, we get:

$$\begin{aligned} {}^b\dot{Q}_{ij} &= ({}^b\dot{R}_f)({}^fQ_{ij}) + ({}^bR_f)({}^fv_j - {}^fv_i) \\ &= -\hat{\omega}_b({}^bR_f)({}^fQ_{ij}) + ({}^bv_j - {}^b v_i) \end{aligned}$$

where ω_b is the angular velocity vector of agent i and for the last equality we have used $\hat{\omega}_b = ({}^bR_f)({}^f\dot{R}_b)$. In the end we get

$${}^b\dot{Q}_{ij} = -\omega_b \times {}^bQ_{ij} + ({}^bv_j - {}^b v_i)$$

which is the relative equation of motion presented in (5).

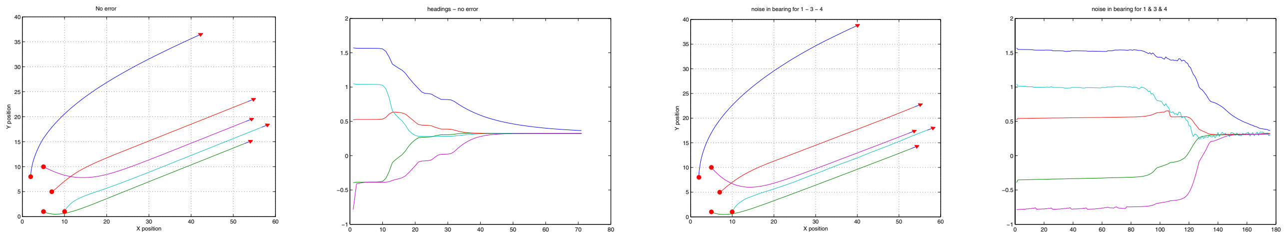

(a) (b) (c) (d)

Fig. 8. The effect of noisy measurements on convergence of the velocity vectors. a,b) ideal case: The trajectories and the heading angles of all agents with the noise-free measurements. c,d) noisy measurements of the bearing decreases the rate of convergence.

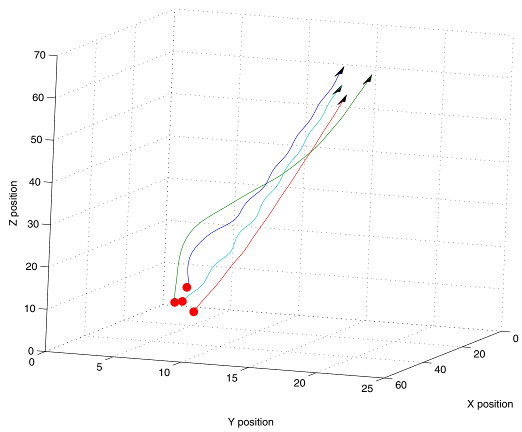

Fig. 6. 4 agents align their velocities in 3D.

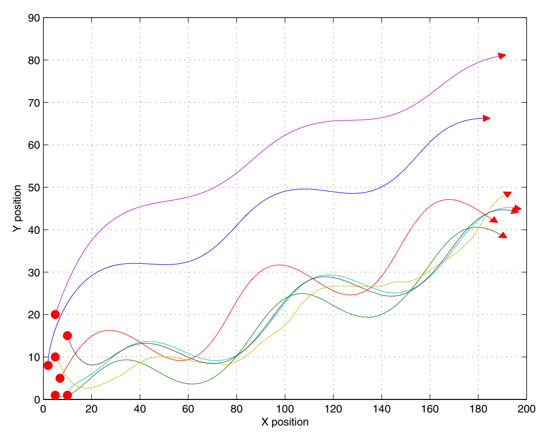

Fig. 7. Agents follow a dynamic leader in 2D.

References

[1] M. Batalin, G.S. Sukhatme, and M. Hattig. Mobile robot navigation using a sensor network. In *IEEE International Conference on Robotics and Automation*, pages 636–642, 2004.

[2] R. W. Beard and V. Stepanyan. Synchronization of information in distributed multiple vehicle coordinated control. In *Proceedings of IEEE Conference on Decision and Control*, December 2003.

[3] S.S. Beauchemin and J.L. Barron. The computation of optical flow. *ACM Computing Surveys*, 27:433–467, 1995.

[4] R. Cipolla and A. Blake. Surface orientation and time to contact from image divergence and deformation. In *Proc. Second European Conference on Computer Vision*, pages 187–202, 1992.

[5] N. Cowan, O. Shakernia, and R. Vidaland S. Sastry. Formation control of nonholonomic mobile robots with omnidirectional visual servoing and motion segmentation. In *IEEE Conference on Intelligent Robotic Systems*, 2003.

[6] A. Das, R. Fierro, V. Kumarand J. Ostrowski, J. Spletzer, and C. J. Taylor. Vision based formation control of multiple robots. *IEEE Trans. Robotics and Automation*, 19:813–825, 2002.

[7] J. Fredslund and M.J. Mataric. A general algorithm for robot formations using local sensing and minimal communication. *IEEE Trans. Robotics and Automation*, pages 837– 846, 2002.

[8] A. Jadbabaie, N. Motee, and M Barahona. On the stability of Kuramoto model of coupled nonlinear oscillators. In *Proceedings of the American Control Conference*, June 2004.

[9] E.W. Justh and P.S. Krishnaprasad. Equilibria and steering laws for planar formations. *Systems and Control letters*, 52(1):25–38, May 2004.

[10] J. J. Koenderink and A. J. van Doorn. How an ambulant observer can construct a model of the enviornment from the geometrical structure of the visual inflow. *Kybernetik*, 1977.

[11] D. N. Lee and P. E. Reddish. Plummeting gannets - a paradigm of ecological optics. *Nature*, 5830:293–294, 1981.

[12] Z. Lin, M. Brouke, and B. Francis. Local control strategies for groups of mobile autonomous agents. *IEEE Transactions on Automatic Control*, 49(4):622–629, April 2004.

[13] N. Moshtagh and A. Jadbabaie. Distributed geodesic control laws for flocking of nonholonomic agents. *IEEE Transaction on Automatic Control*, 2005. submitted.

[14] N. Moshtagh, A. Jadbabaie, and K. Daniilidis. Vision-based distributed coordination and flocking of multi-agent systems. In *Proceedings of Robotics: Science and Systems*, Cambridge, USA, June 2005.

[15] D.J. Naffin, G.S. Sukhatme, and M. Akar. Lateral and longitudinal stability for decentralized formation control. In *Proceedings of the International Symposium on Distributed Autonomous Robotic Systems*, 2004.

[16] N.E. Leonard P. Ogren, E. Fiorelli. Cooperative control of mobile sensing networks: Adaptive gradient climbing in a distributed environment. *IEEE Transaction on Automatic Control*, 49(8):1292–1302, August 2004.

[17] P.E. Rybski, S.A. Stoeter, M. Gini, D.F. Hougen, and N.P. Papanikolopoulos. Performance of a distributed robotic system using shared communications channels. *IEEE Trans. Robotics and Automation*, 19:847–855, 2002.

[18] R. Vidal, O. Shakernia, and S. Sastry. Formation control of nonholonomic mobile robots with omnidirectional visual servoing and motion segmentation. In *IEEE International Conference on Robotics and Automation*, 2003.

[19] W. Wang and Lean-Lacques E. Slotine. On partial contraction analysis for coupled nonlinear oscillators. *Biological Cybernetics*, 2004.

[20] Y. Wang and B. J. Frost. Time to collision is signalled by neurons in the nucleus rotundus of pigeons. *Nature*, 356(6366):236–238, 1992.

[21] T. Weigel, J.-S. Gutmann, M. Dietl, A. Kleiner, and B. Nebel. Cs freiburg: coordinating robots for successful soccer playing. *IEEE Trans. Robotics and Automation*, 19:685– 699, 2002.

[22] Z. Zhu, K. Rajasekar, E. Riseman, and A. Hanson. Panoramic virtual stereo vision of cooperative mobile robots for localizing 3d moving objects. In *IEEE Workshop on Omnidirectional Vision*, pages 29–36, 2000.